

ORIGINAL ARTICLE

Flow cytometry in oral cytology: Improved brush biopsy-based delineation of oral malignant and potentially malignant lesions

Pavithra Srinivasan^{1†}, Sumsum P. Sunny^{1,2†}, Vaishnav Vasudevan¹, Bonney L. James¹, Aditi Hariharan¹, Pramila Mendonca¹, Uma Mohan¹, Subhashini Raghavan³, Shubha Gurudath³, Keerthi Gurushanth³, Ashwini Hallikeri⁴, Vivek Shetty², Vidya Bhushan², Yogesh Dokhe², Naveen B. Shivanand², Satyajit Topajiche⁴, Pavithra Chandrashekhar⁴, Vijay Pillai², Praveen Birur^{1,3}, Christian Brand⁵, Thomas Reiner⁶, Amritha Suresh^{1,2*}, Moni A. Kuriakose^{1,2*}

¹Integrated Head and Neck Oncology Program laboratory, Mazumdar Shaw Medical Foundation, Narayana Health, Bangalore, Karnataka, India

²Department of Head and Neck Oncology, Mazumdar Shaw Medical Center, Narayana Health, Bangalore, Karnataka, India

³Department of Oral Medicine and Radiology, Karnataka Lingayat Education Society's Institute of Dental Sciences, Rajiv Gandhi University of Health Sciences, Bangalore, Karnataka, India

⁴Department of Oral Pathology, Karnataka Lingayat Education Society's Institute of Dental Sciences, Rajiv Gandhi University of Health Sciences, Bangalore, Karnataka, India

⁵Summit Biomedical Imaging LLC, New York, United States of America

⁶Memorial Sloan Kettering Cancer Center, New York, United States of America

[†]These authors contributed equally to this work.

*Corresponding authors:

Amritha Suresh
(amritha.suresh@ms-mf.org)
Moni A Kuriakose
(makuriakose@gmail.com)

Citation: Srinivasan P, Sunny SP, Vasudevan V, *et al.* Flow cytometry in oral cytology: Improved brush biopsy-based delineation of oral malignant and potentially malignant lesions. *J Clin Transl Res.* 2026;12(2):025180023.
doi: 10.36922/JCTR025180023

Received: April 29, 2025

Revised: January 9, 2026

Accepted: February 11, 2026

Published online: April 17, 2026

Copyright: © 2026 Author(s). This is an Open-Access article distributed under the terms of the Creative Commons AttributionNonCommercial 4.0 International (CC BY-NC 4.0), which permits all non-commercial use, distribution, and reproduction in any medium, provided the original work is properly cited.

Publisher's Note: AccScience Publishing remains neutral with regard to jurisdictional claims in published maps and institutional affiliations.

Abstract

Background: Brush biopsy is a minimally invasive method for early detection of oral squamous cell carcinoma (OSCC). Enhanced accuracy for clinical utility depends on analysis of the whole cell population and automated cohort classifications. **Aim:** This study aims to delineate OSCC, high-grade dysplasia (HGD), and low-risk lesions (LRLs) by profiling single-cell level alterations using multiplexed flow cytometry. **Methods:** Brush-biopsy samples were analyzed from patients with LRL, HGD, and OSCC. Flow cytometry analysis was standardized to ascertain cell distribution, heterogeneity, and epithelial cell content. Markers were used for epithelial cell (Pan-Cytokeratin [Pan-CK]/propidium iodide [PI]) and atypical cell (Sambucus-Nigra-Agglutinin-1 [SNA-1]/polyadenosine diphosphate-ribose polymerase inhibitor [PARPi-FL]) delineation. In addition, scatter properties and molecular-equivalence fluorescence (MEF) values of markers were analyzed for cohort classification. **Results:** Brush-biopsy samples from OSCC/HGD patients showed heterogeneity in the percentage of Pan-CK+ve/PI+ve cells. Significant variation in MEF values of SNA-1/PARPi-FL/PI delineated the OSCC cohort (area under the curve > 0.85). Furthermore, the markers in combination with scatter properties delineated OSCC (multivariate logistic regression; sensitivity: 90%, specificity: 82%). The analysis of the forward-scatter height-to-area ratio delineated HGD from low-risk lesions by capturing the morphology-based cellular differences. **Conclusions:** These results suggest that a flow cytometry-based analysis of brush-biopsy samples may serve as an adjunct tool for risk stratification of oral lesions. **Relevance for patients:** This study provides evidence towards the application of flow cytometry as an objective, quantitative adjunct to conventional cytology, and

improves early detection and risk stratification of oral lesions using a minimally invasive sampling method, thereby supporting timely clinical decision-making and patient management.

Keywords: Flow cytometry; Oral cancer; Oral potentially malignant disorders; High-grade dysplasia; FlowCal

1. Introduction

Fluorescence-based imaging techniques that catalogue changes ranging from auto-fluorescence to high-resolution confocal imaging have been applied extensively to detect oral cancer.¹⁻⁶ Considering that 80% of oral cancer arises from oral potentially malignant disorder (OPMD),⁷ detecting high-risk OPMD with an elevated risk of malignant transformation is a significant necessity.⁸⁻¹⁰ An accurate, minimally invasive, pathology-equivalent assay integrated with automated data analysis is needed to detect oral squamous cell carcinoma (OSCC) and high-risk OPMDs. Brush biopsy is a minimally invasive, well-established procedure in cancer screening.¹¹ Yet, techniques to improve its accuracy need to be explored. Molecular cytopathology has been evaluated, and several studies, including ours, have emphasized its significance in delineating high-risk OPMDs.^{12,13} Further development of cell-based methodologies using relevant biomarkers is warranted.

The progression of OPMD is marked by alterations in multiple pathways/processes that can be leveraged for identifying markers for early detection or prognostication. Aberrant glycosylation is a significant process in oral cancer; changes in glycosylation provide a biological basis for differential lectin binding.^{14,15} Lectins, identified for their carbohydrate-binding specificities,^{16,17} are reported to show differential binding in oral epithelial dysplasia.^{18,19} DNA damage response pathways,^{20,21} including those involving poly-(ADP-ribose) polymerase (PARP; DNA repair enzyme), are another significant process in OPMD progression. The presence of upstream molecular mediators that converge to drive these phenotypic changes further strengthens the functional rationale for marker selection. Emerging evidence suggests that microRNAs (miRNAs) play a significant role in oral cancer by regulating pathways involved in glycosylation, DNA damage response, and epithelial transformation.^{22,23} Aberrant miRNA expression has been shown to influence the expression of glycosyltransferases and sialidase enzymes,²⁴⁻²⁶ which leads to altered cell-surface expression of glycoproteins (a hallmark of dysplastic and malignant oral epithelium). Similarly, dysregulation of miRNAs targeting PARP-

related signaling impacts genomic instability and tumor progression, resulting in elevated PARP expression in oral malignancies.^{27,28} In accordance with this evidence, our previous studies on early detection of oral cancer identified that *Sambucus nigra* agglutinin (SNA-1), with a binding site to α -2,6-linked sialic acid, distinguishes high-risk OPMDs by cytology,^{12,29} while a fluorescently-labeled PARP inhibitor (PARPi-FL) is reported to discriminate between biopsied samples of the oral tumor and the surgical margins.²⁷ The adaptation of these markers into novel techniques to improve the accuracy of cell-based early detection needs to be explored.

Marker-integrated assays as an adjunct have improved the detection of atypical cells in cytology.^{13,30,31} A study using DNA image cytometry reported a wide range of sensitivity (16–96.4%) and specificity (90–100%) due to differences in study design, definitions of high- and low-risk lesions, and the protocol used.³² In brush biopsies, analysis of a representative cellular subset from the sample is a limitation; approaches that analyze the entire cell population and integrate automation are essential. Flow cytometry, which analyzes individual cells and provides information on their morphology and marker profiles,³³ has been assessed for clinical applicability in human immunodeficiency virus surveillance, blood cancer phenotyping, and the diagnosis of immunodeficiency diseases.^{34,35} Flow cytometry has also been evaluated for detecting epithelial malignancy.³⁶ However, application of the technique in brush biopsy-based diagnosis has not been explored. There is a critical need for an accurate, minimally invasive, biomarker-based pathology-equivalent assay integrated with automated data analysis; flow cytometry integrated with markers offers a powerful approach toward improving accuracy.

The effectiveness of flow cytometry in identifying atypical cells depends on the specificity of the markers selected; the utility of lectin-based and PARP-targeted markers in a flow cytometry-based analysis of brush biopsy samples has not yet been explored. Together, these molecular alterations manifest as measurable, cell-to-cell variations in surface glycosylation and DNA repair activity, providing a strong biological rationale for the

combined use of lectin-based markers and PARP-targeted markers on a flow cytometry-based platform. The aim of the present study was to evaluate the feasibility of single-cell measurements using SNA-1, PARPi-FL, and scatter properties by flow cytometry-based brush biopsy analysis to delineate OSCC, high-grade dysplasia (HGD), and benign/low-grade dysplastic lesions.

2. Materials and methods

The study was conducted in two phases: the first phase involved standardizing flow cytometry for the identification of atypical cells from brush biopsies, and the second was focused on validating the method for delineating OSCC, HGD (moderate/severe dysplasia), and low-risk lesions (LRL; mild dysplasia, non-dysplasia, normal).

2.1. Study participants and sample collection

The study was conducted at the Head and Neck Oncology Clinic, Mazumdar Shaw Medical Center (approval ID: NHH/MEC-A14/EA/2019) and the Oral Medicine Clinic, Karnataka Lingayat Education Society's Institute of Dental Sciences (approval ID: KLE/JAN 2022/04), Bengaluru, from September 2021 to September 2022. Written informed consent and subject medical history were obtained from eligible participants before enrolment. The inclusion criteria were participants above 18 years of age, clinically diagnosed with suspected benign, OPMD, or oral cancer lesions who had not undergone any prior treatment. Individuals with clinically normal mucosa were recruited as controls. For all lesion cases, brush biopsy samples were obtained before incisional biopsy, and the final lesion classification was based on histopathological confirmation. The subjects with acute illnesses or severe systemic diseases were excluded from the study. Details of risk habit, duration, and cessation were collected. The brush biopsy samples were collected in 1 mL of 70% ethanol for COVID-19 inactivation,^{37,38} followed by 5 min of incubation and centrifugation at 1,100 rpm for 4 min. The pellet was preserved in 1 mL of preservative solution (BD SurePath, BD Biosciences, USA) at 4 °C, prior to processing. The histological diagnosis of the biopsy samples was used as the reference standard for lesion classification (HGD; moderate and severe epithelial dysplasia; LRL; non/mild dysplasia and normal epithelium).³⁹⁻⁴¹

2.2. Flow cytometry-based profiling of brush biopsy samples

The cytometer setup and tracking (CST; CS&T Research Beads, BD Biosciences, USA) beads were taken as an instrument control for instrument setup before starting the experiment. The bead preparation was performed according to the manufacturer's protocol (two drops of CST

beads in 350 µL of sheath fluid). Oral brush biopsy samples consist of epithelial cells along with debris and non-epithelial cells. In the first phase, profiling was conducted to characterize the distribution and heterogeneity of cells. The epithelial cell population was delineated using Pan-Cytokeratin (Pan-CK)⁴² and propidium iodide (PI), while atypical cells were identified using diagnostic markers (SNA-1, PARPi-FL).

For the delineation of epithelial cells, the cellular yield from a brush biopsy was insufficient for standard flow cytometry experiments that require control and compensation steps. Therefore, samples were pooled initially to assess mitigated errors.⁴³ The pooled samples were aliquoted for unstained (control), single staining (Pan-CK, PI), and multiplexing.⁴⁴ Briefly, the samples were permeabilized with 0.1% Triton-x-100 (Himedia Laboratories Pvt. Ltd., India), blocked with 1% bovine serum albumin (30 minutes), and stained with Pan-CK (1:50; Thermo Fisher, USA), and detected using Alexa Fluor-488nm (1:800, 60 minutes; ThermoFisher Scientific, USA). Another aliquot was stained with PI (1:100, 30 minutes; Merck, USA) after permeabilization and blocking. During multiplexing, the samples were stained with Pan-CK followed by PI to distinguish the epithelial cells (Pan-CK⁺PI⁺) from the debris (Pan-CK⁺PI⁻). The experiments were performed using a flow cytometer system (FACS Canto II, BD Biosciences, USA). The unstained population was used for gating/doublet-cell discrimination.

For marker profiling using diagnostic markers, SNA-1/PARPi-FL, diagnostic marker dilutions were optimized in the CAL-27 cell line (moderately differentiated squamous cell carcinoma of the tongue; gift from the Institute of Bioinformatics, Bangalore, India), cultured in Dulbecco's Modified Eagle Medium.⁴⁵ The cells were trypsinized, washed twice with 0.01 M phosphate-buffered saline (PBS; Sigma Aldrich, USA) before staining with PARPi-FL (Summit Biomedical Imaging LLC, New York, USA) for 15 min,⁴⁶ or SNA-1-fluorescein isothiocyanate (FITC) (EY Laboratories, Inc., USA) for 30 min. For multiplex standardization of epithelial cell markers (Pan-CK, PI) with SNA-1 or PARPi-FL, pooled samples (normal, OPMD, oral cancer) were used. The brush biopsy samples were aliquoted for unstained populations, single-marker staining, and multiplexing (Pan-CK-PI with SNA-1 or PARPi-FL). Briefly, samples were stained with SNA-1 or PARPi-FL, followed by Pan-CK (allophycocyanin [APC]-conjugated, 1:100; Thermo Fisher Scientific, USA) and PI. After standardization, multiplexing was further performed on a patient-wise basis. Unstained controls were performed according to the availability of cells (Figure 1A). For each

cohort, the median and interquartile range of total, as well as median epithelial (Pan-CK⁺) percentage, were calculated to characterize sample variability. Samples with fewer than 50 events or low epithelial cell positivity were excluded from analysis to maintain data quality.

2.3. Data analysis from the flow cytometer

The raw data were obtained from the flow cytometry standard (FCS) files using BD FACS DIVA software (V 6.1.1, BD Biosciences, USA) and processed using the

FlowCal Python library (V 1.3.1, University of California, USA).⁴⁷ Briefly, the arbitrary units (a.u.) measured in flow cytometry varied due to instrument drift,⁴⁸ amount and type of samples, hence rainbow beads (BD Biosciences, USA) were used to calibrate a.u. values to molecules of equivalent fluorophore (MEF)⁴⁷ (Figure 1B). The ratios of height (H) and area (A) of forward scatter (FSC) and side scatter (SSC) (Figure 1C) were analyzed for each event. The MEF values of each event were normalized to the geometric mean (Equation 1) of that sample, and outliers

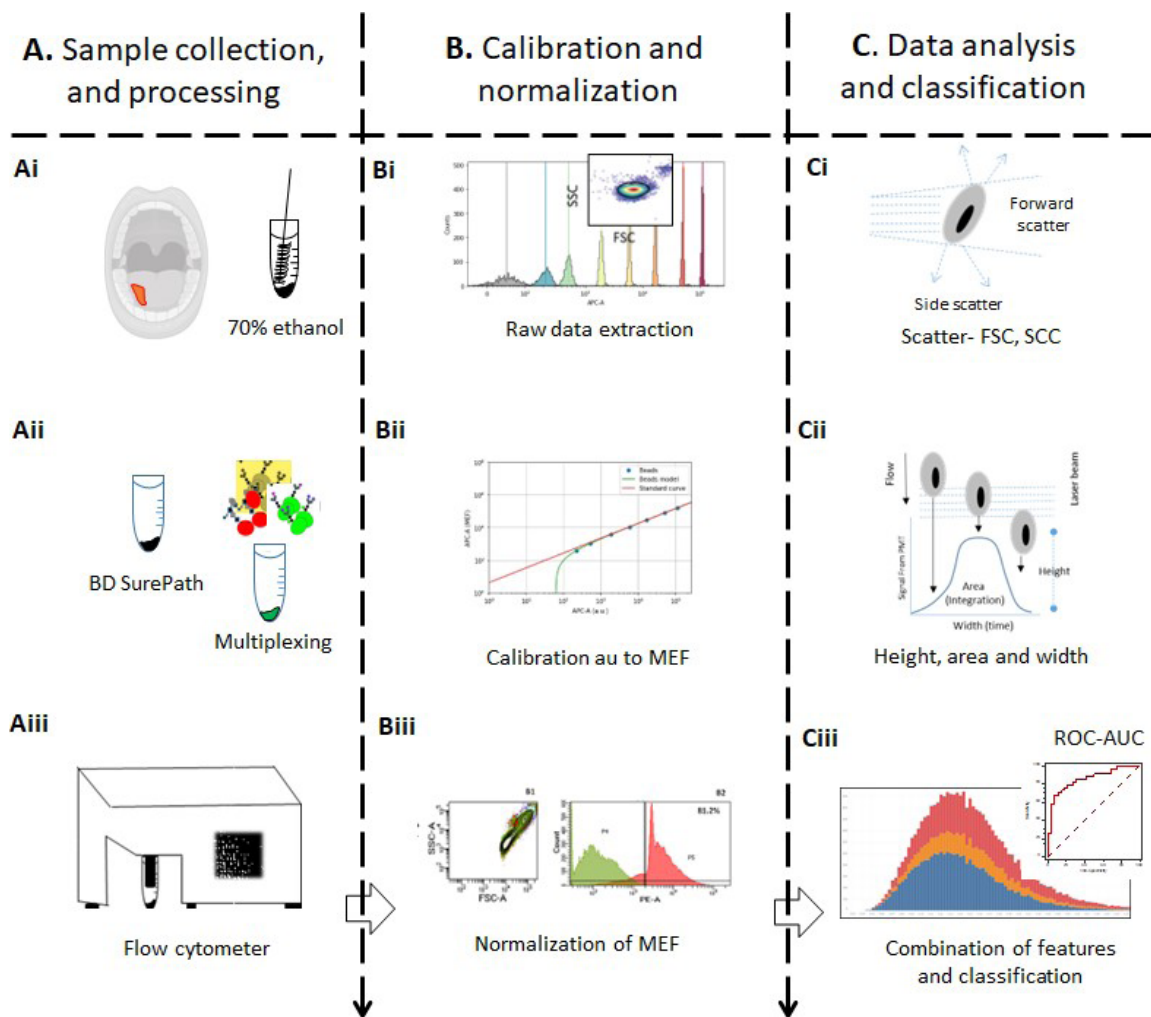


Figure 1. Workflow of the flow cytometry experiment and analysis. Cells were collected from oral lesions in 70% ethanol using a brush biopsy (Ai) and were kept for 10 minutes before being washed twice with phosphate-buffered saline. Subsequently, the cells were stored in BD SurePath (Aii) before multiplexing with diagnostic (SNA-1 or PARPi-FL), epithelial (Pan-CK), and nuclear marker (PI). Flow cytometry experiments were performed using standard methodology (Aiii). The data were obtained from flow cytometry standard files (Bi), and the arbitrary units of fluorescence were calibrated to MEF using rainbow beads (Bi-ii) and negating the values with unstained samples (Biii). The heights and areas of FSC and SSC were obtained along with MEF values (Ci). These features (Cii-Ciii) were utilized to classify LRL, HGD, and OSCC using ROC-AUC.

Abbreviations: AUC: Area under the curve; CI: Confidence interval; FSC: Forward scatter; HGD: High-grade dysplasia; LRL: Low-risk lesion; MEF: Molecular-equivalence fluorescence; OSCC: Oral squamous cell carcinoma; Pan-CK: Pan-Cytokeratin; PARPi-FL: Polyadenosine diphosphate-ribose polymerase inhibitor; PI: Propidium iodide; ROC: Receiver operating characteristics; SNA-1: Sambucus-Nigra-Agglutinin-1; SSC: Side scatter.

were capped using the K3 sigma method.^{49,50} In addition to evaluating the mean fluorescence intensity, analysis was performed using variance-based metrics to capture differences across cell populations in each sample. The variance across the events in the samples was compared between the cohorts for classification.

$$\text{Normalization of MEF} = \frac{\text{MEF of the event} - \text{Geometric mean MEF of sample}}{\text{Geometric mean MEF of sample}} \quad (1)$$

2.4. Statistical analysis

Assuming 80% power (two-sided alpha error 5%), the minimum required sample size was 32 per group for classification. After excluding ineligible samples, 109 samples (number of samples: N_s) were analyzed from 97 participants (number of participants: N_p). Additionally, standardization was performed in another 51 samples (N_p : 38). Descriptive statistics were used to summarize patient demographics, clinical features, and pathology diagnoses. Kolmogorov–Smirnov test was performed to assess the normality of the data. Comparisons were made using the Kruskal–Wallis test, and a two-sided p -value < 0.05 was considered statistically significant. Sensitivity, specificity, receiver operating characteristic (ROC) curve, and multivariate analyses were performed to identify the best features. All statistical analyses were performed using Medcalc (V20.023, MedCalc Software Ltd., Belgium) and Python libraries with FlowCal and pandas libraries (V3.7.4, Python Software Foundation, USA); and figures were generated using Tableau (V2022.2, Tableau Software, USA).

3. Results

3.1. Demographics and clinical details

The brush biopsy samples were collected from 180 oral subsites (Figure 2; N_p : 150). During pre-processing, 20 samples (N_p : 15) (11%) were excluded due to the absence of a cell pellet (Figure 2). Among the 135 participants (age: 21 to 77 years, median: 45), 63% were male; 61% (N_p : 83) of participants had risk habits (tobacco or alcohol) (Table S1). The majority of oral lesions were from the buccal mucosa (N_s : 95; 59%) and the tongue (N_s : 31; 19%).

3.2. Pan-Cytokeratin/propidium iodide delineation of epithelial cells in the brush biopsy samples

The delineation of the epithelial cell population from other cells/debris in brush biopsies was performed using Pan-CK and PI. The unstained sample was used to standardize the gating voltages (FSC = 210, SSC = 270, FITC = 330). In the samples from normal oral mucosa (N_s : 5, pooled for two experiments; number of experiments, N_E : 2) across the two experiments, 30.0% and 69.2% of epithelial cells

(Pan-CK⁺/PI⁺) showed homogenous distribution of the events (Figure 3Ai, Table S2). Pooling samples from OSCC (N_s : 4), OPMD (N_s : 1), and normal (N_s : 3) reduced the percentage positivity of epithelial cells (< 24%) with two distinct clusters, indicating high heterogeneity in the OSCC/OPMD epithelial cell population (N_E : 2; Figure 3Bi, Table S2). Analysis of the markers also revealed that use of Pan-CK alone can lead to a false positivity (Pan-CK⁺/PI⁻) of up to 23.9% (Table S2), indicating the need to use both markers to enumerate the epithelial cell population.

3.3. Profiling of CAL-27 cells with Sambucus-Nigra-Agglutinin-1/polyadenosine diphosphate-ribose polymerase inhibitor-1

Flow cytometric profiling in CAL-27 cells with PARPi-FL (Figure S1A–C) showed an increase in the median percentage positivity (65% to 90%) when a concentration range of 100–500 nM was used. The percentage positivity for SNA-1 at 1:50, 1:25, and 1:10 dilutions were 47.9%, 82.67%, and 96.7%, respectively. No variation in percentage positivity or alteration in expression levels was noted beyond 500 nM PARPi-FL, and 1:25 dilution of SNA-1 resulted in acceptable percentage positivity. Therefore, the subsequent experiments were conducted with the above conditions (Figure S1A–C). The multiplexed profiling of the two markers was assessed in two steps: (i) the oral cells (N_s : 38; N_E : 13) were profiled with SNA-1 or PARPi-FL along with Pan-CK/PI in pooled samples (cohort-wise pooling) to assess heterogeneity, data distribution, and overall positivity; (ii) the samples were assessed patient-wise.

For cohort-wise analysis using SNA-1/Pan-CK/PI staining, a triple-marker (SNA-1⁺Pan-CK⁺PI⁺) positivity of 7.3%, 20.5%, and 31.7% was observed across the three experiments in the cancer cohorts (N_s : 8, N_E : 3). This indicates high, patient-driven, cellular heterogeneity (Figure S2Ai–vi, Table S3). The cohorts also revealed two clusters with differing sizes and granularities. The OPMD pools (N_s : 6, N_E : 2) also showed different clusters, while the percentage of triple-positive cells ranged from 32.9% to 37.1%. The three normal pools (N_s : 8, N_E : 3) showed a homogeneous population of cells with an overall triple positivity of 58.4%, 61.7%, and 70% (Table S3). The difference in median percentage positivity (SNA-1⁺Pan-CK⁺PI⁺) was noticed after compensation (4.2%: range: 0–19.2%; Table S3). The difference in double positive (Pan-CK⁺SNA-1⁺, not using nuclear marker) and triple positive was 0.3% to 61.1%. Increased heterogeneity in the cancer/OPMD cohorts may be attributable to the presence of different epithelial and other cell types.

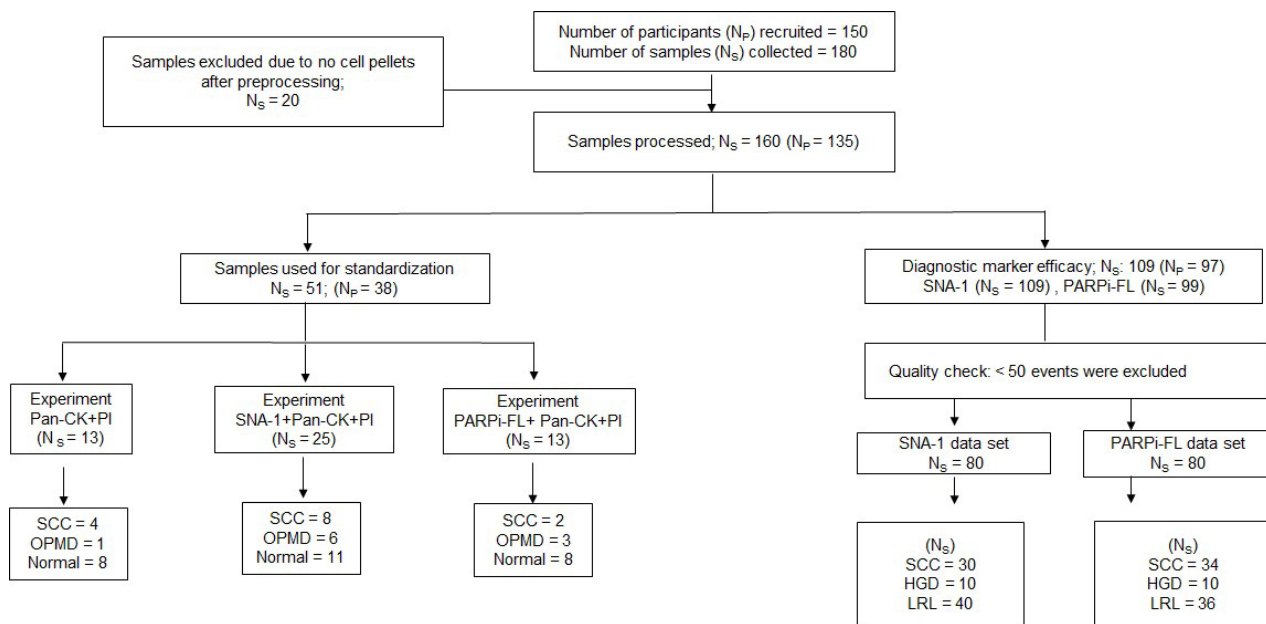


Figure 2. Consort chart of the study. The study collected 180 samples (N_p : 150). Among them, 20 samples (N_p : 15) were excluded due to insufficient pellet size after pre-processing with ethanol, BD SurePath, and phosphate-buffered saline. The standardization was performed on 51 samples (N_p : 38). The profiling was conducted in a stepwise manner to delineate atypical epithelial cells and understand the distribution of cells collected from distinct oral lesions. Initially, the epithelial cells (N_s : 13) were delineated using Pan-CK and PI; atypical cells (N_s : 38) were identified using diagnostic markers (SNA-1, PARPi-FL). Following standardization, pipeline was validated in 109 samples (N_p : 97) for two marker sets (SNA-1/Pan-CK/PI; N_s : 109 and PARPi-FL/Pan-CK/PI; N_s : 99). Samples stored for more than two weeks (SNA-1; N_s : 12, PARPi-FL; N_s : 5) that showed less than 50 events (SNA-1; N_s : 17, PARPi-FL; N_s : 14) were excluded for final analysis.

Abbreviations: HGD: High-grade dysplasia; LRL: Low-risk lesion; OSCC: Oral squamous cell carcinoma; N_p : Number of participants; N_s : Number of samples; Pan-CK: Pan-Cytokeratin; PARPi-FL: Polyadenosine diphosphate-ribose polymerase inhibitor; PI: Propidium iodide; SNA-1: Sambucus-Nigra-Agglutinin-1.

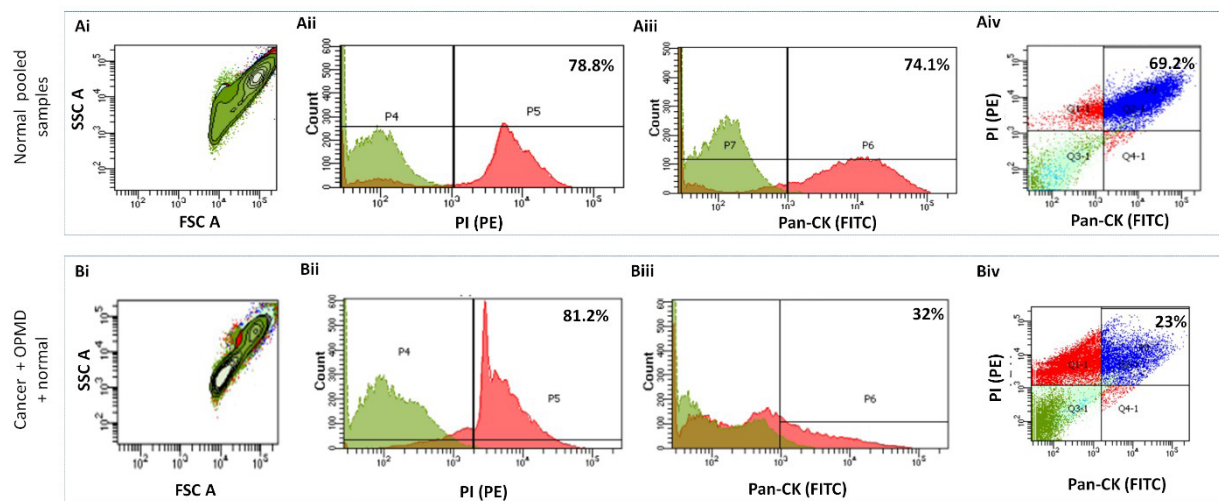


Figure 3. Heterogeneity of brush biopsy samples. (Ai) Forward- and side-scatter dot plots of normal samples showed a homogeneous distribution of cells in a single cluster. The cells collected from normal oral mucosa mainly contained epithelial cells (69.2%). (Aii–Aiv) The difference between PI^{+ve} and $Pan-CK^{+ve}PI^{+ve}$ was less than 10%. (Bi) The heterogeneity of the sample increased when cancer and OPMD cells were pooled with normal cohorts (two clusters). (Bii–Biv) The $Pan-CK^{+ve}PI^{+ve}$ was significantly lower in this cohort, with a difference greater than 50% from PI^{+ve} .

Abbreviations: FITC: Fluorescein isothiocyanate; FSC-A: Forward scatter area; OPMD: Oral potentially malignant disorder; Pan-CK: Pan-Cytokeratin; PE: Phycoerythrin; PI: Propidium iodide; SSC A: Side scatter area.

In cohort-wise analysis with PARPi-FL/Pan-CK/PI staining, PARPi-FL⁺, along with Pan-CK⁺PI⁺, showed a lower positivity range as compared to SNA-1. The cancer pool (N_s : 2, N_e : 1; Figure S2) showed 2.3% positivity, while 8.9% was observed in the OPMD pools (N_s : 3, N_e : 1). The normal pools (N_s : 6, N_e : 3; Figure S2) showed 5.7%, 6.9%, and 20.1% triple marker positivity. The triple-positive cells from the OSCC cohort exhibited a heterogeneous distribution in clusters, as previously observed (Figure S2). Furthermore, as observed in the case of SNA-1, the overall percentage positivity was lower compared to normal cohorts (single cluster), indicating variations in data requiring more granular analysis. The PARPi-FL⁺Pan-CK⁺PI⁺ did not show any changes in percentage positivity after compensation (Table S4).

Given the inherent patient-driven heterogeneity in the samples from OSCC and OPMD, as a final step, the method's efficacy was analyzed individually in an independent cohort of patients (N_p : 97; N_s : SNA-1⁺Pan-CK⁺PI⁺: 109; PARPi-FL⁺Pan-CK⁺PI⁺: 99; Table S5). The age range of participants was 21 to 77 years (median: 45), with the majority of the samples collected from buccal mucosa (N_s : 57). Histological diagnosis categorized the samples as LRL (51%; N_s : 56), HGD (11%; N_s : 12) and OSCC (38%; N_s : 41). Representative histologic images in each cohort are shown in Figure S3. Subsequent quality control excluded 19–29 samples (26.6% for SNA-1 and 19.1% for PARPi-FL) with fewer than 50 events.

Multiplexing with PARPi-FL (Figure S4A), along with Pan-CK/PI (N_s : 80), showed a percentage positivity of 0.3 to 35% (median: 4.3%) in OSCC, 2.2 to 26.3% (median: 11.95%) in HGD, and 0.2 to 60.4% in LRL (median: 4.8%), pointing to a heterogeneous population of atypical cells as observed in the cohort-wise analysis. Similarly, multiplexing with SNA-1 (Figure S4B) along with Pan-CK⁺PI⁺ also showed a wide range of percentage positivity of 0.2 to 60.3% (median: 7.9%) in OSCC, 5.1% to 43.9% in HGD (median: 17.75%), and 0.2% to 74% in LRL (median: 14.25%). An assessment of the number of overall and triple-positive events indicated variability among the patients. The median total events across the SCC, HGD, and LRL cohorts (Figure S4, Table S6) for both SNA-1 and PARPi-FL indicated heterogeneity, which may account for the lack of a significant trend in percentage positivity. Correlation with clinicopathological features indicated that in the OSCC cohort, SNA-1 positivity did not show a significant difference ($p > 0.05$) based on tumor site, T stage, and nodal status (Figure S5Ai–iii), while PARPi-FL percentage positivity was significantly associated with nodal status ($p < 0.05$; Figure S5Bi–iii). The association with tumor differentiation could not be assessed due to

insufficient samples per group.

3.4. Features from triple-positive cells differentiated oral squamous cell carcinoma from high-grade dysplasia and low-risk lesions

To extract features from the triple-positive cells, the arbitrary values of fluorescent channels (FITC, APC, and phycoerythrin) were converted into MEF using FlowCal⁴⁷ regression analysis. The SNA-1 and PARPi-FL datasets were analyzed separately. The distribution of MEF and the scatter ratio (H/A of FSC and SSC) showed increasing counts in each bin with disease progression (Figures S6 and S7).

In SNA-1 data (SNA-1⁺Pan-CK⁺PI⁺), the mean fluorescent intensity of SNA-1 did not differentiate the cohorts (Figure S8Ai). The MEF values of SNA-1 (area under the curve [AUC]: 0.88) and PI (AUC: 0.92) showed significantly higher variance in OSCC ($p < 0.005$, N_s : 30), clearly delineating the cohort (AUC > 0.8) as compared to HGD (N_s : 10) and LRL (N_s : 40). The variance in SNA-1 and PI (Table 1) delineated cancer with higher sensitivity (86.67%; confidence interval [CI]: 69.3–96.2) and specificity (SNA-1 = 80%; CI: 66.3–90; PI = 84%; CI: 70.92–92.8). Furthermore, the variance in FSC-H/A (AUC: 0.87) of the triple-positive cells increased as the disease progressed from LRL to OSCC (Figure 4Ai–iv and Figure 4C). However, the features from the SNA-1 dataset showed less accuracy in delineating HGD from LRL (Figure 4Cii). Multivariate logistic regression analysis indicated that variance in SNA-1, FSC-H/A, and PI was the best combination of features for distinguishing OSCC from HGD/LRL, with a sensitivity of 90% and specificity of 82% (AUC: 0.96; Figure S9).

In the PARPi-FL data (PARPi-FL⁺Pan-CK⁺PI⁺), the MEF values of PARPi-FL showed a significantly higher variance in OSCC ($p < 0.005$, N_s : 34) compared to HGD, while PI MEF values showed a significantly higher variance in OSCC compared to HGD and LRL (Figure 4Bi–ii). There was no significant ($p > 0.05$) difference in the mean fluorescent intensity of PARPi-FL (Figure S8Bi). This variance could in turn categorize the OSCC cohort (AUC > 0.7) as compared to HGD (N_s : 10) and LRL (N_s : 36) with reasonable sensitivity (PARPi-FL = 67.6%, CI: 49.5–82.6; PI = 85.3%, CI: 68.9–95) and specificity (PARPi-FL = 50%, CI: 34.9–65.1, PI = 84.8%, CI: 71.1–93.7). The variance in the FSC-H/A of the triple-positive cells significantly delineated HGD and OSCC from LRL (Figure 4Biii). In multivariate analysis, the MEF variance of PI could delineate OSCC from HGD/LRL (AUC: 0.86) and OSCC/HGD from LRL (AUC: 0.81; Figure S10), indicating the significance of nuclear content variation in atypical cells.

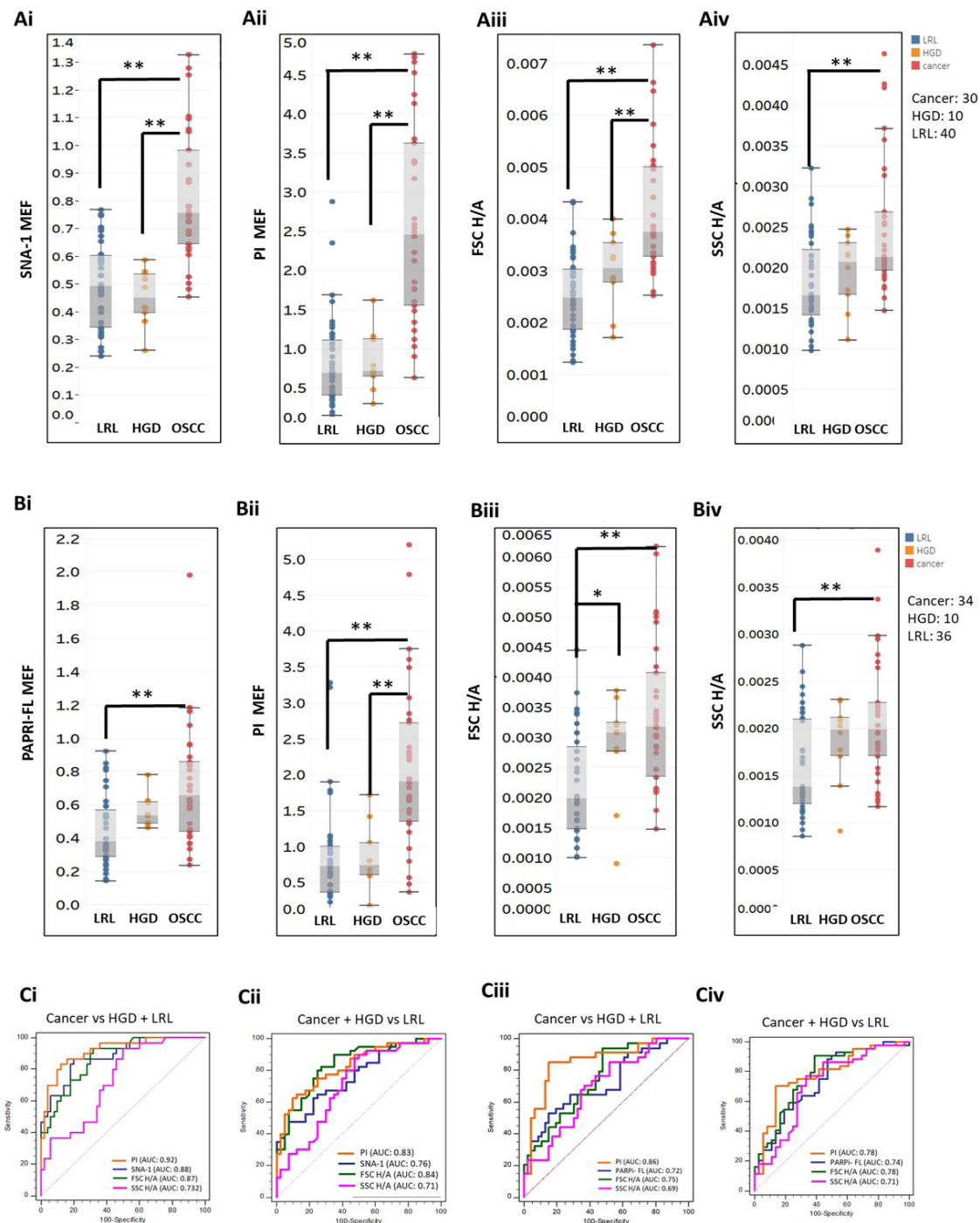


Figure 4. Variance of SNA-1 and PARPi-FL datasets. (Ai–ii, Bi–ii) SNA-1, PARPi-FL, and PI MEF values showed significantly greater variance in OSCC compared to HGD and LRL. The same pattern was noticed in the height-area ratio of forward and side scatter. (Biii) The FSC-H/A increased as the disease progressed, and HGD was significantly different from LRL. Variance in PI-MEF showed the highest ROC-AUC of 0.92 (Ci) and 0.86 (Ciii) in the SNA-1 and PARPi-FL datasets, respectively, in delineating OSCC/HGD. Diagnostic markers also showed the highest AUC (SNA-1: 0.88; PARPi-FL: 0.72). Similarly, FSC-H/A showed the highest AUC in delineating HGD (Cii and Civ). Notes: * $p < 0.05$; ** $p < 0.005$. Abbreviations: AUC: Area under the curve; FSC: Forward scatter; H/A: Height/area ratio; HGD: High-grade dysplasia; LRL: Low-risk lesion; MEF: Molecular-equivalence fluorescence; OSCC: Oral squamous cell carcinoma; PARPi-FL: Polyadenosine diphosphate-ribose polymerase inhibitor; PI: Propidium iodide; ROC: Receiver operating characteristics; SNA-1: Sambucus-Nigra-Agglutinin-1; SSC: Side scatter.

Table 1. Efficacy of features in delineating OSCC, HGD, and LRL in SNA-1 and PARPi-FL datasets

Dataset	Classify	Features	AUC	Sensitivity (95% CI)	Specificity (95% CI)
SNA-1 data	OSCC vs. HGD + LRL	SNA-1	0.884	86.67 (69.3–96.2)	80.00 (66.3–90.0)
		FSC-H/A	0.870	83.33 (65.3–94.4)	70.00 (55.4–82.1)
		PI	0.919	86.67 (69.3–96.2)	84.00 (70.9–92.8)
		SSC-H/A	0.732	80.0 (61.4–92.3)	56.00 (41.3–70.0)
	OSCC + HGD vs. LRL	SNA-1	0.760	80.00 (64.4–90.9)	52.50 (36.1–68.5)
		FSC-H/A	0.837	82.50 (67.2–92.7)	65.00 (48.3–79.4)
		PI	0.826	82.50 (67.2–92.7)	57.50 (40.9–73.0)
		SSC-H/A	0.709	80.00 (64.4–90.9)	57.50 (40.9–73.0)
PARPi-FL data	OSCC vs. HGD + LRL	PARPi-FL	0.717	67.65 (49.5–82.6)	50.00 (34.9–65.1)
		FSC-H/A	0.747	73.53 (55.6–87.1)	54.35 (39.0–69.1)
		PI	0.855	85.29 (68.9–95.0)	84.78 (71.1–93.7)
		SSC-H/A	0.691	70.59 (52.5–84.9)	63.04 (47.5–76.8)
	OSCC + HGD vs. LRL	PARPi-FL	0.741	75.00 (59.7–86.8)	58.33 (40.8–74.5)
		FSC-H/A	0.775	79.55 (64.7–90.2)	63.89 (46.2–79.2)
		PI	0.783	81.82 (67.3–91.8)	58.33 (40.8–74.5)
		SSC-H/A	0.712	77.27 (62.2–88.5)	66.67 (49.0–81.4)

Abbreviations: AUC: Area under the curve; CI: Confidence interval; FSC: Forward scatter; H/A: Height/area ratio; HGD: High-grade dysplasia; LRL: Low-risk lesion; OSCC: Oral squamous cell carcinoma; PARPi-FL: Polyadenosine diphosphate-ribose polymerase inhibitor; PI: Propidium iodide; SNA-1: Sambucus-Nigra-Agglutinin-1; SSC: Side scatter.

In both datasets, the variance in the MEF values of SNA-1 and PARPi-FL highly correlated with the FSC-H/A, indicating the capability of the markers to demarcate the heterogeneous population of cells in the brush biopsies (Spearman's rank correlation: 0.69–0.71; $p < 0.005$; [Figure 5](#)).

4. Discussion

Oral squamous cell carcinomas represent approximately 90% of mouth neoplasms, with a high mortality rate.⁵¹ Early detection is the most efficient way to increase survival. Chronic exposure to carcinogens induces oxidative stress, leading to DNA damage and genomic instability, while activating pro-inflammatory signaling pathways that enhance epithelial cell proliferation and survival.^{52–54} Oxidative stress-driven inflammation also promotes glycosylation reprogramming.^{16,55} Given this axis

in OPMD progression, the choice of markers specifying DNA damage and aberrant glycosylation is extremely significant. In the current study, the multiplexing of molecular markers, SNA-1 (detecting aberrant sialylation) and PARPi-FL (detecting PARP), with cellular scatter parameters (FSC/SSC and FSC-H/FSC-A ratios) enabled flow cytometry-based risk stratification of OSCC and HGD lesions from LRL from brush biopsy samples.

Definitive diagnosis of oral cancer mandates incisional biopsy, while brush biopsy, though minimally invasive, lacks specific diagnostic criteria.^{56,57} Cell-based molecular assays that provide pathology-equivalent diagnoses with an easy readout are invaluable for early detection. Our previous study reported improved sensitivity of cytology in delineating cancer/HGD from LRL.¹² MCRae *et al.*¹³ reported that molecular cytology with machine-learning models achieves 99% accuracy for identifying malignant

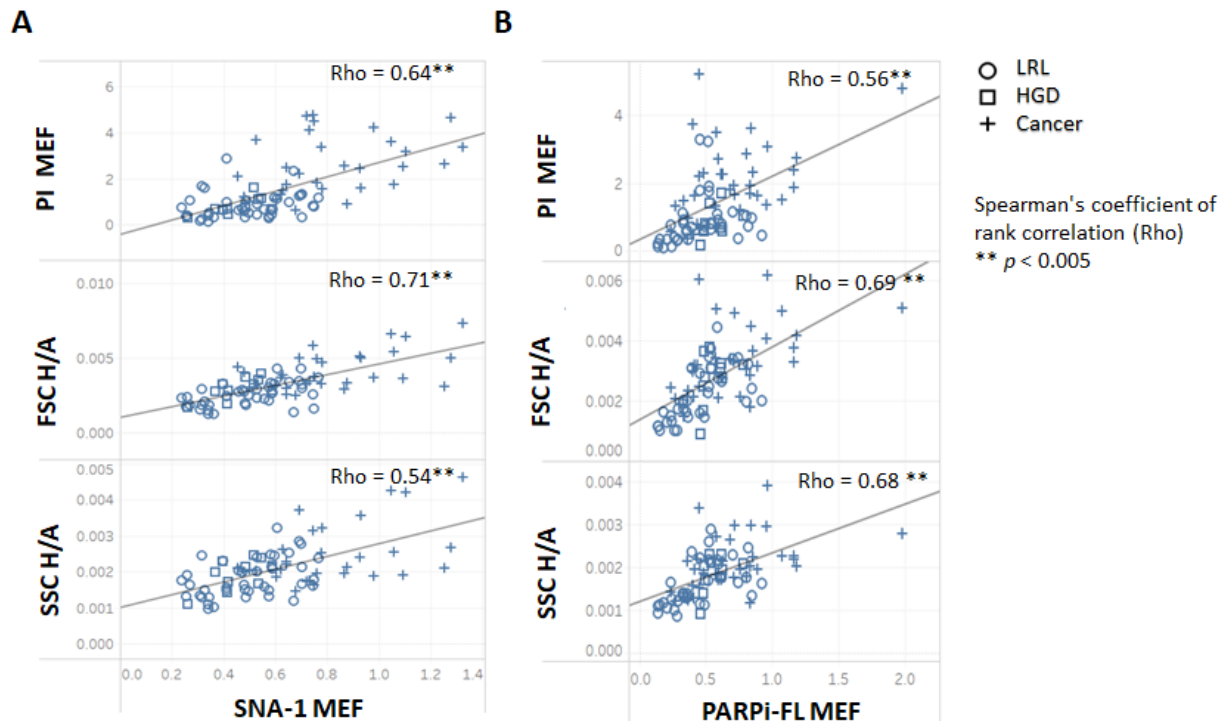


Figure 5. Correlation of diagnostic markers to cellular features. The stacked plot depicted the correlation between the variance of diagnostic markers (SNA-1 and PARPi-FL) and scatter, granularity, and nuclear staining. The variance of nuclear content (PI), size (FSC), and granularity (SSC) significantly correlated with MEF in SNA-1 and PARPi-FL, with the correlation increasing with disease progression (LRL to OSCC). Note: $**p < 0.005$.

Abbreviations: AUC: Area under the curve; CI: Confidence interval; FSC: Forward scatter; H/A: Height/area ratio; HGD: High-grade dysplasia; LRL: Low-risk lesion; MEF: Molecular-equivalence fluorescence; OSCC: Oral squamous cell carcinoma; PARPi-FL: Polyadenosine diphosphate-ribose polymerase inhibitor; PI: Propidium iodide; SNA-1: Sambucus-Nigra-Agglutinin-1; SSC: Side scatter.

lesions. The current study is, to the best of our knowledge, the first to explore flow cytometry-based analysis of brush biopsy samples, aiming to detect oral cancer and high-grade dysplastic lesions. Given that conventional cytology analyses only a representative subset of the brush biopsy sample, flow cytometry, which can assess the entire sample, is a definite advancement. Furthermore, insights into the cellular distributions and morphology/size increase the possibility of investigating the contributions of these parameters to diagnosis. Previously, studies have explored the feasibility of flow cytometry for clinical applications.^{58,59} Our study aims to profile the oral brush biopsies by flow cytometry and assess the significance of detailed cellular measurements obtained. The major challenges were the paucity of cells and the inherent heterogeneity, making it difficult to delineate epithelial cells from the cellular milieu.

Initial standardization in pooled samples provided an insight into the underlying heterogeneity in cancer/OPMDs. This further enabled cohort-wise marker patterning, along with assay optimization, voltage standardization, and assessment of overall marker performance across cohorts, despite limited sample availability. However, we

acknowledge that pooling of samples during the phase may obscure individual variability. Accordingly, all subsequent analyses evaluating diagnostic performance were performed on patient-wise datasets to preserve biological variability. Adopting a strategy akin to the one employed in a recent study that utilized EpCAM,⁶⁰ we used Pan-CK for gating epithelial cells. However, false positives from cell debris in the Pan-CK⁺ population necessitated the use of an additional marker. In our study, while Pan-CK was used to identify epithelial cells, PI was used to exclude debris and non-nucleated material. The double-marker strategy has been previously employed in previous studies for the delineation of a specific cell population.^{61,62} Furthermore, to categorize atypical epithelial cells, we used SNA-1, a marker of abnormal glycosylation, and PARPi-FL, a nuclear marker, based on our previous studies. A triple-marker positivity, which signified the presence of atypical epithelial cells, was therefore used to categorize the patient cohorts.

Analysis of the percentage positivity of epithelial cells using the marker(s) indicated that, contrary to expectations, OSCC samples exhibited a lower proportion

of SNA-1⁺/PARPi-FL⁺ cells compared to OPMD/normal samples, with triple-marker positivity not a significant differentiator between the cohorts. Heterogeneity in the cellular milieu and variability in the number of events were confounding factors as observed in other studies.^{61,63} While OSCC cohorts exhibited a higher number of events with fewer epithelial cells, attributed to blood cell contamination (bleeding from ulcerated lesions), OPMDs showed fewer epithelial cells, possibly due to a thick keratin layer. Conventional flow cytometry, which infers overall percentage positivity, is challenging for analyzing brush biopsy samples due to inherent variability in cell counts, fluorescence a.u., and high heterogeneity. These results may be attributed to biological and technical factors intrinsic to malignant lesions. Conceptually, carcinogen-induced changes are reflected in the OSCC cohort in a non-homogeneous and context-dependent manner at the single-cell level. The changes lead to heterogeneous populations characterized by necrotic/apoptotic debris, context-dependent cellular glycosylation, nuclear fragmentation, and chromatin disruption that impair PARPi-FL/SNA-1 binding. Furthermore, tumor-associated inflammation and stromal infiltration may mask epithelial epitopes, collectively contributing to reduced marker positivity.⁶⁴⁻⁶⁶ Together, these processes lead to extensive heterogeneity in cell-based profiles as opposed to uniform shifts in expression. Technically, pre-analytical variables also influence fluorescence-based readouts. Standardization in brush biopsy sample collection (repeated strokes until a blood tinge appears), storage media/duration (Surepath, 2 weeks), and selection of epithelial cells (Pan-CK/PI) ensured homogeneity in our protocol. Nevertheless, the loss of 20 samples due to insufficient cells and fluorescence variability suggested that storage or fluorophore quenching may have affected binding efficiency and signal intensity. These findings suggest that ensuring epithelial yield/homogeneity in sample collection (including brushing force/number of strokes), staining, and marker-based cell enrichment are essential pre-requisites to confirm that the heterogeneity is biology-driven. In this study, to overcome the challenges of heterogeneity, measurement parameters based on MEF values calibrated with FlowCal⁴⁷ were used for differentiating the oral lesions. This strategy of raw data obtained from FCS files for a more comprehensive analysis has previously been used for normalization and calibration.⁶⁷⁻⁶⁹

The analysis of SNA-1 with Pan-CK/PI, based on MEF value, significantly delineated OSCC from other lesions but was not significant for HGD, possibly due to low sample sizes. The features from the PARPi-FL dataset (FSC-H/A), however, could delineate HGD from LRL. Significantly, the variance in this marker expression, along

with the size parameters, was the distinguishing feature between the cohorts. Previous studies using the markers in cytology/histology samples indicated higher accuracy for SNA-1¹² and PARPi-FL⁶ in delineating HGD, which is why these markers were chosen. In our study, although the percentage positivity was not a distinguishing factor, accounting for heterogeneity in cellular features improved the detection efficacy of HGD (AUC: 0.81–0.86). The difference was possibly due to the high sensitivity of flow cytometry in detecting heterogeneity and/or the modified sample collection protocol mandated due to the pandemic. Nevertheless, minimally invasive methods to delineate HGD, the lesions with the highest susceptibility to malignant transformation, represent a significant advancement in addressing a major challenge in oral cancer screening and surveillance: accurate risk stratification for timely clinical management. The current workflow demonstrates feasibility in a research setting; its implementation in low-resource or large-scale screening settings requires scalability, instrument accessibility, and consideration of the costs associated with post-acquisition normalization using tools such as FlowCal. Future optimization, including streamlined acquisition pipelines, simplified normalization strategies, and the development of portable or point-of-care flow-based platforms, can facilitate incorporation into clinical workflows.

Atypical cells are characterized by morphological changes in size and cellular architecture, which are leveraged by the pathologists.⁷⁰ These parameters can be correlated with FSC (size) and SSC (granularity). When incorporated into the analysis pipeline, the results indicated that the OSCC cohort exhibited high variation in the FSC of atypical cells (SNA-1⁺Pan-CK⁺PI⁺), which could delineate the cohort from HGD/LRL (AUC: 0.87) and LRL (AUC: 0.83), showing the significance of heterogeneity in atypical cells. This is in accordance with a previous study, which reported that cell size parameters decrease as the disease progresses from LRL to cancer, as indicated by an increased H/A.⁴¹ Pleiomorphism, apoptotic cells, and ploidy are other features that are reflected in the FSC-H/A, which acts as a surrogate marker of cell size abnormalities.^{41,71} The correlation of PI staining with nuclear content/DNA ploidy has been reported previously.⁷² In this study, PI expression (MEF value from triple-marker-positive cells) increased as the disease progressed from LRL to cancer, and the values could differentiate the cohorts with high accuracy (OSCC vs. HGD/LRL; AUC: 0.85–0.92). This evidence indicates that integrating marker profiles with morphological features from flow cytometric data delineates OSCC/HGD from LRLs. The scatter- and fluorescence-derived morphological features captured by flow cytometry also revealed high heterogeneity. The FSC-H/FSC-A ratios,

along with MEF values of SNA-1 and PARPi-FL, were significant discriminators, emphasizing that variance measurements are most relevant for delineating brush biopsy samples.

The limitations of this study include a paucity of samples for flow cytometric evaluation, which necessitated the pooling approach during standardization. Furthermore, conventional cytological evaluation could not be performed in parallel with flow cytometry, and histopathological diagnosis was used as the reference standard. Although specific SOPs were designed and followed for the study, 20 specimens were excluded due to low event counts. Variability in cellular yield and epithelial representation was another challenge; blood contamination/RBC depletion, particularly in OSCC samples, contributed to sample heterogeneity and may have impaired marker-specific signal detection. These factors emphasize the need for standardized brushing techniques, optimized collection media, and improved sample-processing workflows in flow cytometry-based studies. Additionally, the relatively modest sample size, particularly within the HGD subgroup, may have constrained statistical power for certain comparisons and warrants cautious interpretation of subgroup-specific findings. Furthermore, owing to the limitations of the brush biopsy technique, sub-epithelial/stromal changes could not be documented.

Future studies should focus on larger, multicentre cohorts to improve statistical robustness and validate scatter-based parameters for HGD detection. Integration of additional molecular markers, improved multiplexing strategies, and the evaluation of portable or point-of-care cytometry platforms may further enhance clinical feasibility. Longitudinal studies assessing lesion progression and outcome prediction would also be valuable for establishing the role of flow cytometry as a screening and risk-stratification tool in OPMDs.

5. Conclusion

In the current study, multiplexed flow cytometry using the SNA-1-PARPi-FL-PI combination, specifying the alterations in DNA damage and aberrant glycosylation, revealed high cellular heterogeneity that increased with disease severity. The heterogeneity measure (MEF variance) of the cells was a determinant of malignancy and a significant discriminator of OSCC patients (sensitivity/specificity > 80%). Furthermore, the variance in the FSC-H/A of the triple-positive cells significantly distinguished HGD and OSCC from LRL, whereas multivariate analysis indicated that nuclear variations (as detected by PI) were significant in delineating OSCC from HGD/LRL. This study indicates that individual cell-based measurements

reflect non-uniform, context-dependent changes in cellular processes, cataloguing distribution factors and high-resolution measurement of cellular size/granularity. The ability to measure the entire cell population by flow cytometry is a significant advancement in delineating brush biopsy samples. Although the challenges include the need for higher cell numbers, heterogeneity in cell types, and the need for multiplexed profiling, its application in the screening/early detection setting can be made clinically viable using a handheld/portable alternative. Clinical application for delineation of HGD/OSCC in high-risk populations will be highly significant for identifying lesions amenable to biopsy, treatment, and/or monitoring. However, further assessment and validation are needed, especially for the delineation of HGD to establish the efficiency of flow cytometry in large-scale screening either independently or as an adjunct to conventional/molecular cytopathology.

Acknowledgments

We acknowledge the Mazumdar Shaw Medical Foundation for its support in facility usage. We acknowledge Ms. Mythri C and Ms. Shivani for formatting and uploading the documents.

Funding

This study was supported by the Biotechnology Industry Research Assistance Council, India (<https://birac.nic.s/>; GCE-India/R4/2018/006) under the Grand Challenges Explorations program.

Conflict of interest

The authors declare no conflict of interest.

Author contributions

Conceptualization: Thomas Reiner, Amritha Suresh, Moni A Kuriakose

Data curation: Pavithra Srinivasan, Sumsum P. Sunny, Aditi Hariharan, Vaishnav Vasudevan, Bonney L. James, Satyajit Topajiche, Uma Mohan, Pavithra Chandrashekhar, Vijay Pillai, Praveen Birur, Amritha Suresh

Formal analysis: Pavithra Srinivasan, Sumsum P. Sunny, Aditi Hariharan, Uma Mohan, Vaishnav Vasudevan, Bonney L. James, Amritha Suresh, Pramila Mendonca, Subhashini Raghavan, Shubha Gurudath, Keerthi Gurushanth, Vivek Shetty, Vidya Bhushan R, Yogesh Dokhe, Naveen B. Shivanand, Ashwini Hallikeri

Investigation: Sumsum P. Sunny, Pramila Mendonca, Subhashini Raghavan, Shubha Gurudath, Keerthi Gurushanth, Vivek Shetty, Vidya Bhushan, Yogesh

Dokhe, Naveen B. Shivanand, Ashwini Hallikeri

Methodology: Christian Brand, Thomas Reiner, Amritha Suresh, Moni A Kuriakose, Pavithra Srinivasan, Sumsum P. Sunny, Aditi Hariharan, Vaishnav Vasudevan, Bonney L. James, Satyajit Topajiche, Uma Mohan, Pavithra Chandrashekhar, Vijay Pillai, Praveen Birur

Writing-original draft: Pavithra Srinivasan, Sumsum P. Sunny, Vaishnav Vasudevan, Bonney L. James

Writing-review & editing: Amritha Suresh, Moni A Kuriakose, Christian Brand, Vijay Pillai, Praveen Birur, Thomas Reiner

Ethics approval and consent to participate

The study received ethical approval from the institutional ethics committees of Mazumdar Shaw Medical Center (NHH/MEC-A14/EA/2019) and Karnataka Lingayat Education Society's Institute of Dental Sciences (KLE/JAN-2022/04), Bengaluru, and written informed consent was obtained from all participants prior to enrolment.

Consent for publication

Written informed consent was obtained from all participants for the publication of anonymized data.

Availability of data

The datasets generated during the current study are available from the corresponding author on reasonable request. Processed data are provided in the figures and tables.

References

- Messadi DV. Diagnostic aids for detection of oral precancerous conditions. *Int J Oral Sci.* 2013;5(2):59-65. doi: 10.1038/ijos.2013.24
- Giovannacci I, Vescovi P, Manfredi M, Meleti M. Non-invasive visual tools for diagnosis of oral cancer and dysplasia: A systematic review. *Med Oral Patol Oral Cir Bucal.* 2016;21(3):e305-e315. doi: 10.4317/medoral.20996
- Fedele S. Diagnostic aids in the screening of oral cancer. *Head Neck Oncol.* 2009;1:5. doi: 10.1186/1758-3284-1-5
- Mendonca P, Sunny SP, Mohan U, Birur NP, Suresh A, Kuriakose MA. Non-invasive imaging of oral potentially malignant and malignant lesions: A systematic review and meta-analysis. *Oral Oncol.* 2022;130:105877. doi: 10.1016/j.oraloncology.2022.105877
- Demetrio de Souza Franca P, Kossatz S, Brand C, *et al.* A phase I study of a PARP1-targeted topical fluorophore for the detection of oral cancer. *Eur J Nucl Med Mol Imaging.* 2021;48(11):3618-3630. doi: 10.1007/s00259-021-05372-6
- Kossatz S, Pirovano G, Demetrio De Souza Franca P, *et al.* Validation of the use of a fluorescent PARP1 inhibitor for the detection of oral, oropharyngeal and oesophageal epithelial cancers. *Nat Biomed Eng.* 2020;4(3):272-285. doi: 10.1038/s41551-020-0526-9
- Kumari P, Debta P, Dixit A. Oral Potentially Malignant Disorders: Etiology, Pathogenesis, and Transformation Into Oral Cancer. *Front Pharmacol.* 2022;13:825266. doi: 10.3389/fphar.2022.825266
- Felthaus O, Ettl T, Gosau M, *et al.* Cancer stem cell-like cells from a single cell of oral squamous carcinoma cell lines. *Biochem Biophys Res Commun.* 2011;407(1):28-33. doi: 10.1016/j.bbrc.2011.02.084
- Patel SS, Shah KA, Shah MJ, Kothari KC, Rawal RM. Cancer stem cells and stemness markers in oral squamous cell carcinomas. *Asian Pac J Cancer Prev.* 2014;15(20):8549-8556. doi: 10.7314/apjcp.2014.15.20.8549
- Laprise C, Shahul HP, Madathil SA, *et al.* Periodontal diseases and risk of oral cancer in Southern India: Results from the HeNCe Life study. *Int J Cancer.* 2016;139(7):1512-1519. doi: 10.1002/ijc.30201
- Idrees M, Farah CS, Sloan P, Kujan O. Oral brush biopsy using liquid-based cytology is a reliable tool for oral cancer screening: A cost-utility analysis: Oral brush biopsy for oral cancer screening. *Cancer Cytopathol.* 2022;130(9):740-748. doi: 10.1002/cncy.22599
- Sunny SP, D RR, Hariharan A, *et al.* CD44-SNA1 integrated cytopathology for delineation of high grade dysplastic and neoplastic oral lesions. *PLoS One.* 2023;18(9):e0291972. doi: 10.1371/journal.pone.0291972
- McRae MP, Modak SS, Simmons GW, *et al.* Point-of-care oral cytology tool for the screening and assessment of potentially malignant oral lesions. *Cancer Cytopathol.* 2020;128(3):207-220. doi: 10.1002/cncy.22236
- Dabelsteen E. Cell surface carbohydrates as prognostic markers in human carcinomas. *J Pathol.* 1996;179(4):358-369. doi: 10.1002/(SICI)1096-9896(199608)179:4<358::AID-PATH564>3.0.CO;2-T
- Vigneswaran N, Peters KP, Hornstein OP, Diepgen TL. Alteration of cell surface carbohydrates associated with

- ordered and disordered proliferation of oral epithelia: a lectin histochemical study in oral leukoplakias, papillomas and carcinomas. *Cell Tissue Kinet.* 1990;23(1):41-55.
doi: 10.1111/j.1365-2184.1990.tb01108.x
16. Pinho SS, Reis CA. Glycosylation in cancer: mechanisms and clinical implications. *Nat Rev Cancer.* 2015;15(9):540-555.
doi: 10.1038/nrc3982
17. Strome A, Kossatz S, Zanoni DK, Rajadhyaksha M, Patel S, Reiner T. Current Practice and Emerging Molecular Imaging Technologies in Oral Cancer Screening. *Mol Imaging.* 2018;17:1536012118808644.
doi: 10.1177/1536012118808644
18. Mazumdar S, SenGupta SK, Param R, Sinha SN. Binding pattern of eight different lectins in healthy subjects and patients with dysplastic and malignant lesions of the oral cavity. *Int J Oral Maxillofac Surg.* 1993;22(5):301-305.
doi: 10.1016/s0901-5027(05)80521-1
19. Pillai KR, Remani P, Kannan S, *et al.* Lectin histochemistry of oral premalignant and malignant lesions: correlation of JFL and PNA binding pattern with tumour progression. *Eur J Cancer B Oral Oncol.* 1996;32B(1):32-37.
doi: 10.1016/0964-1955(95)00051-8
20. Li Y, Tong Y, Liu J, Lou J. The Role of MicroRNA in DNA Damage Response. *Front Genet.* 2022;13:850038.
doi: 10.3389/fgene.2022.850038
21. Wang Y, Taniguchi T. MicroRNAs and DNA damage response: implications for cancer therapy. *Cell Cycle.* 2013;12(1):32-42.
doi: 10.4161/cc.23051
22. Lajer CB, Garmaes E, Friis-Hansen L, *et al.* The role of miRNAs in human papilloma virus (HPV)-associated cancers: bridging between HPV-related head and neck cancer and cervical cancer. *Br J Cancer.* 2012;106(9):1526-1534.
doi: 10.1038/bjc.2012.109
23. Manikandan M, Deva Magendhra Rao AK, Arunkumar G, *et al.* Oral squamous cell carcinoma: microRNA expression profiling and integrative analyses for elucidation of tumorigenesis mechanism. *Mol Cancer.* 2016;15(1):28.
doi: 10.1186/s12943-016-0512-8
24. Agrawal P, Kurcon T, Pilobello KT, *et al.* Mapping posttranscriptional regulation of the human glycome uncovers microRNA defining the glycode. *Proc Natl Acad Sci USA.* 2014;111(11):4338-4343.
doi: 10.1073/pnas.1321524111
25. Ibrahim SA, Hassan H, Gotte M. MicroRNA regulation of proteoglycan function in cancer. *FEBS J.* 2014;281(22):5009-5022.
doi: 10.1111/febs.13026
26. Thomas D, Rathinavel AK, Radhakrishnan P. Altered glycosylation in cancer: A promising target for biomarkers and therapeutics. *Biochim Biophys Acta Rev Cancer.* 2021;1875(1):188464.
doi: 10.1016/j.bbcan.2020.188464
27. Kossatz S, Weber W, Reiner T. Detection and Delineation of Oral Cancer With a PARP1-Targeted Optical Imaging Agent. *Mol Imaging.* 2017;16:1536012117723786.
doi: 10.1177/1536012117723786
28. Wang F, Gouttia OG, Wang L, Peng A. PARP1 Upregulation in Recurrent Oral Cancer and Treatment Resistance. *Front Cell Dev Biol.* 2021;9:804962.
doi: 10.3389/fcell.2021.804962
29. Sunny SP, Khan AI, Rangarajan M, *et al.* Oral epithelial cell segmentation from fluorescent multichannel cytology images using deep learning. *Comput Methods Programs Biomed.* 2022;227:107205.
doi: 10.1016/j.cmpb.2022.107205
30. Mello FW, Melo G, Guerra ENS, Warnakulasuriya S, Garnis C, Rivero ERC. Oral potentially malignant disorders: A scoping review of prognostic biomarkers. *Crit Rev Oncol Hematol.* 2020;153:102986.
doi: 10.1016/j.critrevonc.2020.102986
31. Scott IS, Odell E, Chatrath P, *et al.* A minimally invasive immunocytochemical approach to early detection of oral squamous cell carcinoma and dysplasia. *Br J Cancer.* 2006;94(8):1170-1175.
doi: 10.1038/sj.bjc.6603066
32. Datta M, Laronde D, Palcic B, Guillaud M. The role of DNA image cytometry in screening oral potentially malignant lesions using brushings: A systematic review. *Oral Oncol.* 2019;96:51-59.
doi: 10.1016/j.oraloncology.2019.07.006
33. McKinnon KM. Flow Cytometry: An Overview. *Curr Protoc Immunol.* 2018;120:5.1.1-5.1.11.
doi: 10.1002/cpim.40
34. Barnett D, Walker B, Landay A, Denny TN. CD4 immunophenotyping in HIV infection. *Nat Rev Microbiol.* 2008;6(11 Suppl):S7-S15.
doi: 10.1038/nrmicro1998
35. Grewal RK, Chetty M, Abayomi EA, Tomuleasa C, Fromm JR. Use of flow cytometry in the phenotypic diagnosis of hodgkin's lymphoma. *Cytometry B Clin Cytom.* 2019;96(2):116-127.

- doi: 10.1002/cyto.b.21724
36. Gaur G, Awasthi NP, Gupta A, *et al.* Diagnostic accuracy of flow cytometry in detecting malignant epithelial cells in serous effusions. *J Am Soc Cytopathol.* 2023;12(6):423-435.
doi: 10.1016/j.jasc.2023.09.003
 37. Chen CC, Chi CY. Biosafety in the preparation and processing of cytology specimens with potential coronavirus (COVID-19) infection: Perspectives from Taiwan. *Cancer Cytopathol.* 2020;128(5):309-316.
doi: 10.1002/cncy.22280
 38. Straccia P, Rossi ED, Martini M, *et al.* Description of a new biosafe procedure for cytological specimens from patients with COVID-19 processed by liquid-based preparations. *Cancer Cytopathol.* 2020;128(12):905-909.
doi: 10.1002/cncy.22341
 39. Birur PN, Patrick S, Warnakulasuriya S, *et al.* Consensus guidelines on management of oral potentially malignant disorders. *Indian J Cancer.* 2022;59(3):442-453.
doi: 10.4103/ijc.IJC_128_21
 40. Khan AS, Khan ZA, Nisar M, *et al.* Description of clinicopathological characteristics of oral potentially malignant disorders with special focus on two histopathologic grading systems and subepithelial inflammatory infiltrate. *J Cancer Res Ther.* 2023;19(Suppl 2):S724-S730.
doi: 10.4103/jcrt.jcrt_969_22
 41. Sunny S, Baby A, James BL, *et al.* A smart tele-cytology point-of-care platform for oral cancer screening. *PLoS One.* 2019;14(11):e0224885.
doi: 10.1371/journal.pone.0224885
 42. Lopresti A, Malergue F, Bertucci F, *et al.* Sensitive and easy screening for circulating tumor cells by flow cytometry. *JCI Insight.* 2019;4(14):e128180.
doi: 10.1172/jci.insight.128180
 43. Drescher H, Weiskirchen S, Weiskirchen R. Flow Cytometry: A Blessing and a Curse. *Biomedicines.* 2021;9(11):1613.
doi: 10.3390/biomedicines9111613
 44. Finak G, Langweiler M, Jaimes M, *et al.* Standardizing Flow Cytometry Immunophenotyping Analysis from the Human ImmunoPhenotyping Consortium. *Sci Rep.* 2016;6:20686.
doi: 10.1038/srep20686
 45. Tadijan A, Humphries JD, Samarzija I, *et al.* The Tongue Squamous Carcinoma Cell Line Cal27 Primarily Employs Integrin alpha6beta4-Containing Type II Hemidesmosomes for Adhesion Which Contribute to Anticancer Drug Sensitivity. *Front Cell Dev Biol.* 2021;9:786758.
doi: 10.3389/fcell.2021.786758
 46. Kossatz S, Brand C, Gutiontov S, *et al.* Detection and delineation of oral cancer with a PARP1 targeted optical imaging agent. *Sci Rep.* 2016;6:21371.
doi: 10.1038/srep21371
 47. Castillo-Hair SM, Sexton JT, Landry BP, Olson EJ, Igoshin OA, Tabor JJ. FlowCal: A User-Friendly, Open Source Software Tool for Automatically Converting Flow Cytometry Data from Arbitrary to Calibrated Units. *ACS Synth Biol.* 2016;5(7):774-780.
doi: 10.1021/acssynbio.5b00284
 48. Le Lann L, Jouve PE, Alarcon-Riquelme M, *et al.* Standardization procedure for flow cytometry data harmonization in prospective multicenter studies. *Sci Rep.* 2020;10(1):11567.
doi: 10.1038/s41598-020-68468-3
 49. Lehmann R. 3 σ -Rule for Outlier Detection from the Viewpoint of Geodetic Adjustment. *J Surv Eng.* 2013;139(4):157-165.
doi: 10.1061/(asce)su.1943-5428.0000112
 50. Kanamori E, Itoh M, Tojo N, Koyama T, Nara N, Tohda S. Flow cytometric analysis of Notch1 and Jagged1 expression in normal blood cells and leukemia cells. *Exp Ther Med.* 2012;4(3):397-400.
doi: 10.3892/etm.2012.633
 51. Gonzalez-Moles MA, Aguilar-Ruiz M, Ramos-Garcia P. Challenges in the Early Diagnosis of Oral Cancer, Evidence Gaps and Strategies for Improvement: A Scoping Review of Systematic Reviews. *Cancers (Basel).* 2022;14(19):4967.
doi: 10.3390/cancers14194967
 52. Mittal M, Siddiqui MR, Tran K, Reddy SP, Malik AB. Reactive oxygen species in inflammation and tissue injury. *Antioxid Redox Signal.* 2014;20(7):1126-1167.
doi: 10.1089/ars.2012.5149
 53. Rembalkowska N, Kocik Z, Klosinska A, *et al.* Inflammation-Driven Genomic Instability: A Pathway to Cancer Development and Therapy Resistance. *Pharmaceuticals (Basel).* 2025;18(9):1406.
doi: 10.3390/ph18091406
 54. Huang R, Zhou PK. DNA damage repair: historical perspectives, mechanistic pathways and clinical translation for targeted cancer therapy. *Signal Transduct Target Ther.* 2021;6(1):254.
doi: 10.1038/s41392-021-00648-7
 55. Pillitteri LJ, Guo X, Dong J. Asymmetric cell division in plants: mechanisms of symmetry breaking and cell fate determination. *Cell Mol Life Sci.* 2016;73(22):4213-4229.
doi: 10.1007/s00018-016-2290-2
 56. Mohanta A, Mohanty PK, Parida G. Cytomorphometric analysis of keratinized round cells in human oral carcinoma. *J Cytol.* 2015;32(2):107-112.

- doi: 10.4103/0970-9371.160561
57. Remmerbach TW, Meyer-Ebrecht D, Aach T, *et al.* Toward a multimodal cell analysis of brush biopsies for the early detection of oral cancer. *Cancer*. 2009;117(3):228-235.
doi: 10.1002/cncy.20028
 58. Peters JM, Ansari MQ. Multiparameter flow cytometry in the diagnosis and management of acute leukemia. *Arch Pathol Lab Med*. 2011;135(1):44-54.
doi: 10.5858/2010-0387-RAR.1
 59. Betters DM. Use of Flow Cytometry in Clinical Practice. *J Adv Pract Oncol*. 2015;6(5):435-440.
doi: 10.6004/jadpro.2015.6.5.4
 60. Bockerstett KA, Wong CF, Koehm S, Ford EL, DiPaolo RJ. Molecular Characterization of Gastric Epithelial Cells Using Flow Cytometry. *Int J Mol Sci*. 2018;19(4):1096.
doi: 10.3390/ijms19041096
 61. Tinnevelt GH, Kokla M, Hilvering B, *et al.* Novel data analysis method for multicolour flow cytometry links variability of multiple markers on single cells to a clinical phenotype. *Sci Rep*. 2017;7(1):5471.
doi: 10.1038/s41598-017-05714-1
 62. Schmid I, Dagarag MD, Hausner MA, *et al.* Simultaneous flow cytometric analysis of two cell surface markers, telomere length, and DNA content. *Cytometry*. 2002;49(3):96-105.
doi: 10.1002/cyto.10163
 63. Gough A, Stern AM, Maier J, *et al.* Biologically Relevant Heterogeneity: Metrics and Practical Insights. *SLAS Discov*. 2017;22(3):213-237.
doi: 10.1177/2472555216682725
 64. Diaz-Cano SJ. Tumor heterogeneity: mechanisms and bases for a reliable application of molecular marker design. *Int J Mol Sci*. 2012;13(2):1951-2011.
doi: 10.3390/ijms13021951
 65. Parshenkov A, Hennet T. Glycosylation-Dependent Induction of Programmed Cell Death in Murine Adenocarcinoma Cells. *Front Immunol*. 2022;13:797759.
doi: 10.3389/fimmu.2022.797759
 66. Kurkalang S, Roy S, Acharya A, *et al.* Single-cell transcriptomic analysis of gingivo-buccal oral cancer reveals two dominant cellular programs. *Cancer Sci*. 2023;114(12):4732-4746.
doi: 10.1111/cas.15979
 67. Fedorec AJH, Robinson CM, Wen KY, Barnes CP. FlopR: An Open Source Software Package for Calibration and Normalization of Plate Reader and Flow Cytometry Data. *ACS Synth Biol*. 2020;9(9):2258-2266.
doi: 10.1021/acssynbio.0c00296
 68. Rutter JW, Ozdemir T, Galimov ER, *et al.* Detecting Changes in the *Caenorhabditis elegans* Intestinal Environment Using an Engineered Bacterial Biosensor. *ACS Synth Biol*. 2019;8(12):2620-2628.
doi: 10.1021/acssynbio.9b00166
 69. Beal J, Overney C, Adler A, Yaman F, Tiberio L, Samineni M. TASBE Flow Analytics: A Package for Calibrated Flow Cytometry Analysis. *ACS Synth Biol*. 2019;8(7):1524-1529.
doi: 10.1021/acssynbio.8b00533
 70. Jara-Lazaro AR, Thamboo TP, Teh M, Tan PH. Digital pathology: exploring its applications in diagnostic surgical pathology practice. *Pathology*. 2010;42(6):512-518.
doi: 10.3109/00313025.2010.508787
 71. Baeten J, Johnson A, Sunny S, *et al.* Chairside molecular imaging of aberrant glycosylation in subjects with suspicious oral lesions using fluorescently labeled wheat germ agglutinin. *Head Neck*. 2018;40(2):292-301.
doi: 10.1002/hed.24943
 72. Sasikumar J, Laha S, Naik B, Das SP. Enhanced visualization of nuclear staining and cell cycle analysis for the human commensal *Malassezia*. *Sci Rep*. 2024;14(1):20936.
doi: 10.1038/s41598-024-69024-z